



Research article

Phytofabrication of silver nanoparticles using callus extracts of natural tetraploid *Trifolium pratense* L. and its bioactivities

Havva Karahan^{*1} , Nurten Tetik² , Hatice Colgecen¹ 

¹ Zonguldak Bulent Ecevit University, Faculty Science, Department of Biology, 67100, Zonguldak, Türkiye

² Yildiz Technical University, Faculty of Chemistry and Metallurgy, Department of Food Engineering, 34000, Istanbul, Türkiye

Abstract

One of the main subjects of plant biotechnology is plant tissue culture and in recent years is considered a possible approach model for green and eco-friendly biosynthesis of nanoparticles. This study aimed to present calli produced from the natural tetraploid *Trifolium pratense* L. containing high amounts of phenolic compounds and glycosidic bioactive macromolecules and the biosynthesis of silver nanoparticles from calli. Combinatorial optimization of silver nanoparticles was achieved for the first time in this study, thanks to the stabilizing and reducing properties of hypocotyl, apical meristem, and epicotyl derived callus extracts of the natural tetraploid *T. pratense* L. biosynthesized nanoparticles from three different callus extracts. Callus extracts were used to create different experiments with AgNO₃ at various concentrations (0.16, 0.5, 0.84, 1.18, 1.52 and 1.96 mg L⁻¹), different temperatures (40, 50, 60, 70, 80, 90, 100°C), and different pH levels (5, 7, 10) to carry out the biosynthesis of AgNPs. Biologically synthesized AgNPs were easily monitored by color change in ultraviolet and UV-Vis spectroscopy proved to be a fast and simple method. Also, TEM, XRD, and FTIR analyses were done to characterize and confirm the formation of crystalline nanoparticles. It was determined that antibacterial activity inhibition was achieved by using the Agar-well diffusion method for antibacterial activity measurements on Gram-positive *Staphylococcus aureus* ATCC 25923 and Gram-negative *Escherichia coli* CECT 4972 bacteria. Biosynthesized AgNPs were observed in the wavelength range of 400-500 nm in the UV-VIS spectrum. TEM analysis demonstrated the size and shape of biosynthesized silver nanoparticles under different conditions. It was observed that the smaller silver nanoparticles were spherical and the larger silver nanoparticles were triangular, elliptical, and spherical shape. The XRD analysis proved the presence of Ag₀ in nanoparticles and showed crystal structure for silver nanoparticles. By FTIR analysis, O-H hydroxyl groups of functional groups on the AgNP surface, H-linked OH stretching, C-H stretching, -CH stretching of -CH₂ and -CH₃ functional groups, C-N and carboxylate, aliphatic phosphate and primary amine stretching were expressed. Biosynthesized silver nanoparticles showed antibacterial activity against Gram-positive *S. aureus* ATCC 25923 bacteria, AgNP hypocotyl (1.7mm), AgNP-epicotyl (1.1mm) against Gram-negative *E. coli* CECT 4972 bacteria. Among the hypocotyl, apical meristem, and epicotyl callus cultures, the highest antioxidant activity was observed in the AgNPs obtained from hypocotyl-concentration experiments, with a DPPH radical activity of 52% and an ABTS radical activity of 68%. In conclusion, these findings underscore the potential of biotechnological strategies in green nanotechnology, which can be offered for developing metal nanoparticles with potential biomedicine and biotechnology applications.

Keywords: Antibacterial activity; antioxidant activity; callus culture; characterization; reducing and stabilizing agents; silver nanoparticles

* Corresponding author.

E-mail address: havva01030@gmail.com (H. Karahan).

<https://doi.org/10.51753/flsrt.1357092> Author contributions

Received 08 September 2023; Accepted 15 December 2023

Available online 30 December 2023

2718-062X © 2023 This is an open access article published by Dergipark under the [CC BY](https://creativecommons.org/licenses/by/4.0/) license.

1. Introduction

Nanobiotechnology is an important and rapidly developing field that allows interdisciplinary studies such as medicine, drug delivery, biomedical, physics, biology, chemistry, and materials engineering with an environmentally friendly approach (Pandit, 2015; Anjum and Abbasi, 2016; Aktepe, 2021). It increases the chance of economic production by making sensitive and rapid applications that positively affect the diagnosis and treatment of diseases. Increasing knowledge of cell and intracellular communication will bring the scientific world to the next level very quickly with the help of nanotechnological methods.

Silver nanoparticles (AgNP), the product of this study, are used in food packaging, wastewater treatment, and textile industry, but are most commonly used in biomedical practices (Salem and Fouda, 2021). For example, AgNPs function in biosensing, imaging, and drug delivery. At the same time, AgNPs increase attention due to their antibacterial activities and cost-effective preparations (Yurttas et al., 2022). They are cytotoxic agents and are used in antimicrobial, anti-cancer, anti-inflammatory (Gonzalez et al., 2017) or wound care applications (Aziz et al., 2014; Kumar and Kathireswari, 2016; Singh et al., 2016; Xia et al., 2016; Tian et al., 2018). The current interest is in the antiviral activity of AgNPs because of the COVID-19 pandemic (Jeremiah et al., 2020; Allawadhi et al., 2021).

To increase the scientific areas in which AgNPs can be used, different synthesis methods have been tried to be developed, recently. The most common approach using chemical reducing agents to synthesize AgNPs is chemical reduction. One of these methods is *in vitro* AgNP biosynthesizing with plant tissue cultures. Callus production with plant tissue culture techniques can be carried out with an explant of the plant (from leaf, shoot, root or hypocotyl, epicotyl, cotyledon, apical meristem or young first leaves) and continuous production can be achieved. In addition, with plant tissue culture techniques under controlled conditions will be carried out, secondary metabolites prevent the plant from being exposed to biotic and abiotic stress factors (Ochoa-Villarreal et al., 2016; Ozyigit et al., 2023). Callus extracts contain different amounts of biochemicals, which are reducing and stabilizing agents, and contain many polar groups, which are very important for the stabilization of AgNPs. The natural tetraploid *Trifolium pratense* L. used in our study is rich in flavonoids, so this study evaluated the biosynthesis of AgNPs by callus extracts.

Natural tetraploid *T. pratense* L. can be grown widely in the Eastern Anatolia Region and Black Sea Regions of Türkiye (Elci, 1982). The chromosome number of natural tetraploid *T. pratense* L. is $2n=4x=28$ (Buyukkartal and Colgecen, 2007). The natural tetraploid *T. pratense* L. variety contains more secondary metabolites than the diploid variety of the plant (Khaosaad et al., 2008; Colgecen et al., 2014). Especially, due to the isoflavones it contains, its phytoestrogenic activity is very high. The reasons for choosing the natural tetraploid *T. pratense* L. callus extracts as reducing and stabilizing agents are its richness of essential phytochemicals and its medicinal effects. In our previous study, some secondary metabolites obtained from calli were analysed and high amounts of secondary metabolites were determined (Colgecen et al., 2014).

In nanobiotechnology, silver nanoparticles are better than gold and copper nanoparticles. AgNPs exhibit antibacterial properties in many ways; (1) the microbial cell surface is effective to adhere of AgNPs, it causes alteration of transport activity and cell membrane damage, and AgNPs interact with

cellular organelles of microbial cells and biomolecules which affect the corresponding cellular mechanism (2) AgNPs increase in ROS in microbial cells and so, begin damage in cell (3) AgNPs arrange the cellular signaling system, resulting in cell death (Dakal et al., 2016).

According to literature studies, common agents of wound infections are *Staphylococcus aureus* and *Escherichia coli*. The cause of hospital-acquired infections is *S. aureus* that is one of the five most common, and both community-acquired and hospital acquired staphylococcal infections are increasing. The various diseases ranging from subacute superficial skin infection to life-threatening septicemia such as food poisoning, skin infection, bacteremia and bone/joint infection are agent effected from *S. aureus*. In community-acquired urinary tract infections, the highest rate of *E. coli* is isolated as an infectious agent in urine cultures. Considering that drug-resistant *S. aureus* and *E. coli* are emerging rapidly but there is no antibiotic development line, alternative methods are needed to fight these antibiotic resistant bacteria (Li et al., 2011; Avcioglu et al., 2019).

Antibiotic resistance is defined as some strains of a microorganism species being unaffected by an antibiotic or an antibiotic-sensitive strain becoming resistant by one of several resistance mechanisms. In addition, the World Health Organization (WHO) explains that if the problem of resistance to antibiotics is not resolved, each year will cause 10 million deaths due to drug-resistant diseases by 2050 and devastating damage to the economy because of the global financial crisis of 2008-2009 (World Health Organization, 2019). Economically (whether directly linked to agriculture or livestock), it is predicted that antimicrobial resistance will push up to 24 million people into high poverty by 2030 (Arsène et al., 2021).

There are no studies in the literature on the use of hypocotyl, apical meristem and epicotyl derived callus extracts of natural tetraploid *T. pratense* L. as a biological source for AgNP biosynthesis. This study focuses on AgNPs biosynthesis using extracts from the natural tetraploid *T. pratense* L. calli. and is the first report. The presence of AgNPs was determined by UV-visible spectroscopy, TEM, FTIR, and XRD analyses. Additionally, it was aimed at developing an effective method against *S. aureus* and *E. coli* using biosynthesized AgNPs. It was determined that the DPPH and ABTS radical scavenging activity of biosynthesized AgNPs.

2. Materials and methods

2.1. Preparation of callus extracts

Natural tetraploid *T. pratense* L. was grown in an experiment garden (41.45124°N, 31.76037°W) that belongs to the Biology Department, Science Faculty, Zonguldak Bulent Ecevit University. The seeds were collected in May 2021. To create aseptic seedlings, firstly, surface sterilization of naturally tetraploid *T. pratense* L. seeds collected annually was performed, the seeds were treated with 10% sodium hypochlorite (NaOCl) solution for 10 minutes and then rinsed with distilled water 3 times. (Colgecen et al., 2008; Colgecen et al., 2014). After surface sterilization, 6-7 seeds of natural tetraploid *T. pratense* L. were germinated in MS (Murashige and Skoog, 1962) nutrient medium without plant growth regulator. Hypocotyl (0.5 cm), apical meristem (2-3 mm), and epicotyl (0.5 cm) explants of 15-day-old aseptic seedlings were taken in MS medium containing plant growth regulators: kinetin (1.5 mg L⁻¹), NAA (1.5 mg L⁻¹), and 2,4-D (0.7 mg L⁻¹) (Colgecen et al.,

2014). It is solidified with 20 g L⁻¹ sucrose, 0.7% g agar, and pH adjusted at 5.8. The culture was incubated at a photoperiod of 16/8 h, and the temperature was set to 24±1°C (irradiation with 37 μmol m⁻² s⁻¹ and 2000 lux was provided by cool-white fluorescent tubes).

The induced callus was friable and yellow. Calli were subcultured every 4 weeks. Photographs were taken under a stereo microscope (Leica EZ4D). The hypocotyl, apical meristem, and epicotyl derived calluses obtained from the second subculture were weighed at 10 g and taken into a 250 ml Erlenmeyer flask. 100 ml of sterile distilled water was added, and the flask was then shaken in an 80°C water bath at 180 rpm for one hour (Anjum and Abbasi, 2016; Xia et al., 2016; Aref and Salem, 2020). When the temperature reached room temperature, the extracts were filtered by a Whatman No. 1, and the volume of the filtrate was made up to 100 ml with distilled water (Lashin et al., 2021; Ahmad et al., 2022). Thus, 1 g/10 ml of extract was obtained. The extracts were stored at +4±1°C in the dark.

2.2. Green synthesis of silver nanoparticles

10 mL of natural tetraploid *T. pratense* L. extract was taken from 1 g/10 ml stock extract and was mixed with different concentrations (0.16, 0.5, 0.84, 1.18, 1.52, and 1.96 mg L⁻¹, separately and respectively) of freshly prepared silver nitrate aqueous solution (AgNO₃) for the biosynthesis of AgNPs (Lashin et al., 2021). They were incubated at 24°C±2 and under daylight. It took 6, 24, and 48 hours for the reduction of silver ions. A color change of red was observed in the reaction mixture after the incubation period. According to the UV-visible spectrophotometer results, since the fastest reduction and the fastest color change occurred at 1.96 mg L⁻¹ AgNO₃, temperature and pH experiments were continued with 1.96 mg L⁻¹ AgNO₃.

To confirm the biosynthesis of AgNPs, 10 ml of hypocotyl, apical meristem, and epicotyl derived callus extracts were added to 1.96 mg L⁻¹ AgNO₃ (Fluka) aqueous solution at different temperatures (40-50-60-70-80-90-100°C). In order to evaluate AgNPs biosynthesis in different pH ranges (5-7-10), 10 mL of extracts were adjusted to 5, 7, and 10 with 1N HCl and 1M NaOH, respectively. Then 1.96 mg L⁻¹ AgNO₃ was added to the prepared solutions (Nabikhan et al., 2010; Anjum and Abbasi, 2016; Xia et al., 2016; Yugay et al., 2023). The first pH of hypocotyl, apical meristem, and epicotyl derived callus extracts was 5.89, 6.00, and 5.92, respectively.

2.3. Characterization of bio-silver nanoparticles

UV-visible spectroscopy analysis was performed with a UV-visible absorption spectrophotometer (Tetra T80+UV/VIS Spectrophotometer PG) to determine the formation of AgNPs biosynthesized from calli. After mixing the callus extracts with AgNO₃, the formation of AgNPs was first visually observed and confirmed by color change. Absorbance measurements in the range of 200 to 800 nm were then recorded to distinguish the maximum surface plasmon of AgNPs. The analyses were carried out with quartz cuvettes. Distilled water was used for blank and zero UV-visible spectroscopy (Aref and Salem, 2020; Lashin et al., 2021).

The size and shape distribution of AgNPs was performed with a TEM (Hitachi HT7800) device operating at an acceleration voltage of 120 kV (Rakesh et al., 2022). AgNPs,

which are biosynthesis products, were centrifuged at 12.000 rpm for 10 minutes. All callus extract residues and unconverted Ag(I) ions were washed three times with distilled water. Finally, it was sonicated in distilled water for 5 minutes. It was filtered with 0.22 μm filters. 3 μl of sample was dropped on the carbon-coated grid. All samples were dried at 24°C±2 for 15 min.

Phase formation, purity, and crystal structure of the biosynthetic product AgNPs were identified using XRD (X-ray diffraction) spectrometry (Panalytical Empyrean). The process was carried out using Cu/Kα radiation (λ = 1.54 Å) at a value of 2θ between 20° and 80°. The tube current of 40 mA, scan speed of 0.1°/min, step size of 0.02°, and voltage of 45 kV were maintained as operating parameters (Ozturk Kup et al., 2020; Gharari et al., 2022). AgNPs, which are biosynthesis products, were centrifuged at 25.000 rpm for 7 minutes. All plant extract residues and unconverted Ag(I) ions were washed three times with distilled water. Then, samples were dried at 24±2°C for 2 days.

Perkin Elmer 400 FTIR/FTFIR Spectrometer Spotlight 400 was used for FTIR (Fourier Transform Infrared Spectroscopy) spectroscopy. The wavelength was measured at a resolution of 4 cm⁻¹ in the range of 400 to 4000 cm⁻¹ according to ATR (Lashin et al., 2023). The callus aqueous extract's functional groups, which have major roles in the biosynthesis of AgNPs, were analyzed using FTIR. AgNPs, which are biosynthesis products, were centrifuged at 12.000 rpm for 10 minutes. All plant extract residues and unconverted Ag(I) ions were washed three times with distilled water. Then, samples were dried at 60°C for 48 hours (Sharifi-Rad et al., 2020; Lashin et al., 2021).

XRD and FTIR analyses were carried out at the Science and Technology Application and Research Center, Zonguldak Bulent Ecevit University. TEM analyses were carried out at the Eskisehir Osmangazi University Application and Research Center, Eskisehir.

2.4. Determination of potential biological activity

Antibacterial activity: The agar-well diffusion method was used to determine the antibacterial activity of biosynthesized AgNPs on Gram-positive *S. aureus* ATCC 25923 and Gram-negative *E. coli* CECT 4972 bacteria. Antibacterial levels were tested by inhibition zone measurement. Bacteria were inoculated in 5 mL of TSB medium and incubated at 35±1°C for 18±2 hours. After incubation, 0.1 ml of the bacterial culture adjusted to 0.5 McFarland standards was evenly spread on Mueller-Hinton agar. Then, 8 mm diameter wells were made in Petri dishes using sterile punches at 2.5 cm intervals, and 100 μL of samples diluted to a final concentration of 1 μg/1μl were placed in each trough and incubated at 37°C for 24 hours. The inhibition zone (ZOI) was evaluated in terms of the diameter of the growth-free regions with the aid of a caliper. As a negative control, sterile distilled water was used (Devi et al., 2018; Baruah et al., 2021; EUCAST, 2022). The antibacterial tests were repeated three times, and the average of the three obtained data points was reported.

2.5. In vitro antioxidant assay: 2,2-diphenyl-1-picrylhydrazyl (DPPH)

The activity of DPPH in the samples was determined by making some modifications to the Sanchez-Moreno method (Wang and Lee, 1996). The DPPH activity of biosynthesized AgNPs was studied against 2,2-diphenyl-1-picrylhydrazyl

(DPPH). Extracts of hypocotyl, apical meristem, and epicotyl derived callus were used as a control group. Biosynthesized AgNPs from the extracts were prepared from aqueous products at different concentrations (1.0, 0.5, 0.25, and 0.125 mg L⁻¹) and added to a well plate. Then, 2 ml of freshly prepared ethanolic solution of DPPH solution was added to each well (Szydłowska-Czerniak et al., 2012; Fierascu et al., 2014). The plate was incubated in the dark for approximately 30 minutes. At this time, the mixing solution changed from violet to yellow. With a UV-spectrophotometer, 3 repetitive readings were performed at 1-minute intervals at an absorbance of 517 nm. A butylated hydroxyanisole (BHA) solution was used as a standard. The Tetra Brand T80+UV/VIS Spectrometer PG Instruments Model was used to determine DPPH free radical scavenging activity.

DPPH activity was calculated as Ellnain et al. (2003) and Ozturk Kup et al. (2020):

$$\text{Inhibition\%} = [\text{Control (DPPH)} - \text{Sample (DPPH)}] / \text{Control (DPPH)} \times 100.$$

2.6. In vitro antioxidant assay of 2,2'-azinobis-(3-ethylbenzothiazoline-6-sulfonic acid) (ABTS)

The ABTS free radical scavenging activities of the samples were determined by making some modifications to the method studied by Moldovan et al. (2016). To form ABTS⁺ radical cation, 6.5 mM ABTS, and 2.45 mM potassium persulfate solution were mixed in equal volumes (1:1) and incubated for 16 hours in the dark and at room temperature until a dark green color appeared. ABTS⁺ was diluted with distilled water to give an absorbance value of 0.6-0.8 units at 734 nm (Moldovan et al., 2016; Sharifi-Rad et al., 2021). Extracts of hypocotyl, apical meristem, and epicotyl derived callus were used as a control group. Different amounts of AgNP aqueous products (1.0, 0.5, 0.25, and 0.125 mg L⁻¹) were prepared and added to a well plate. Then, a freshly prepared aqueous solution of 2 mL ABTS was added to each well. The plate was incubated in the dark for approximately 30 minutes. Also, the mixing solution changed from dark purple to transparent. Three repetitive readings were performed at 1-minute intervals at 734 nm absorbance with a UV spectrophotometer. BHA solution was used as a standard. The Tetra Brand T80+UV/VIS Spectrometer PG Instruments Model was used to evaluate ABTS free radical scavenging activity.

ABTS radical scavenger percentage was calculated with the equation $\% = [\text{Control (ABTS)} - \text{Sample (ABTS)}] / \text{Control (ABTS)} \times 100$ (Das et al., 2020).

The Scherer-Debye equation was used to calculate the average crystallite size of AgNPs (Eq. 2):

$$D = (K \times \lambda) / \beta \times \cos \theta$$

D= the size of the crystal, its unit is equal to λ unit, usually angstrom or nm,

λ = the X-ray wavelength, Used K-Alpha1 wavelength,

K= a dimensionless shape factor, with a value close to unity,

B= the full width at half maximum,

θ = the peak position on the horizontal axis of diffraction pattern, which, if the horizontal axis is 2θ . It should be divided into two to get θ .

2.7. Statistical analysis

A statistical analysis of the data given in callus percentages was attributed to the previous study (Colgecen et al., 2014). They subjected the percentages of callus to the arcsin

transformation (Snedecor and Cochran, 1967) and analyzed all the data statistically with the SPSS package program. AgNPs biosynthesis was performed from the callus extracts of natural tetraploid *T. pratense* L.; each experiment was repeated 3 times. For the statistical analysis and calculations of the differences between the radical scavenging activities of the obtained AgNPs products, "SPSS for Windows Ver. 24.0" (SPSS Inc., Chicago, IL., USA) package programs the groups were compared with the Duncan separation test (Duncan, 1955). In statistical decisions, the $p < 0.05$ level was accepted as an indicator of a significant difference.

3. Results

3.1. Callus initiation

The seeds of the natural tetraploid *T. pratense* L. (Fig. 1a) were germinated in an MS nutrient medium without a plant growth regulator. The first germination was observed after 3 days. Hypocotyl (0.5 cm), apical meristem (2-3 mm), and epicotyl (0.5 cm) explants (Fig. 1c) of grown 15-day-old aseptic seedlings (Fig. 1b) were planted in MS media (Colgecen et al., 2014). Hypocotyl, apical meristem, and epicotyl derived calli were obtained after four weeks (Fig. 2).

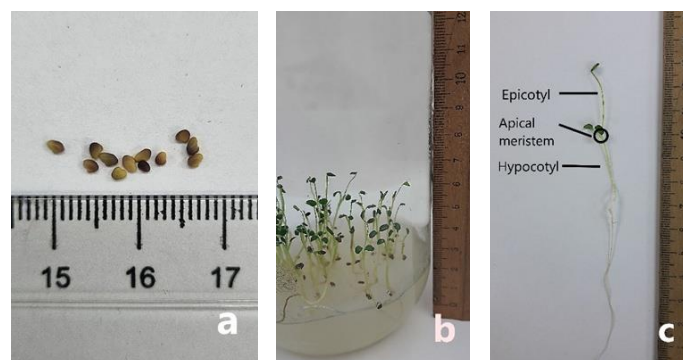


Fig. 1. Natural tetraploid *T. pratense* L. (a) seeds, (b) 15-day-old aseptic seedlings in *in vitro*, (c) parts of a 15-day-old aseptic seedling.



Fig. 2. The four weeks calli producing from natural tetraploid *T. pratense* L. (a) apical meristem, (b) epicotyl, (c) hypocotyl.

3.2. Ultraviolet-violet spectroscopy

AgNPs were produced by mixing 1.96 mg L⁻¹ AgNO₃ with 10 ml of hypocotyl, apical meristem, and epicotyl derived callus extracts. The reduction of Ag⁺ in the AgNO₃ solution and the formation of AgNPs were determined using UV-vis spectroscopy, which is one of the important techniques. The occurrence of biosynthesized AgNPs was visualized with a color change (dark red-brown) after completion of the reaction between extracts of hypocotyl, apical meristem, and epicotyl derived callus with 1.96 mg L⁻¹ AgNO₃ (Fig. 3). The biosynthesized AgNPs maximum absorbance was visualized for hypocotyl, apical meristem, and epicotyl derived callus at wavelengths of 470, 458, and 460 nm, respectively. The change

of $1.96 \text{ mg L}^{-1} \text{ AgNO}_3 + 1 \text{ g}/10 \text{ ml}$ callus extract in terms of AgNPs formation at 6, 24, and 48 hours was recorded (Fig. 4). The dark red-brown color of the AgNP solution produced with $1.96 \text{ mg L}^{-1} \text{ AgNO}_3$ remained unchanged for 6 months. This demonstrated the stability of AgNPs.

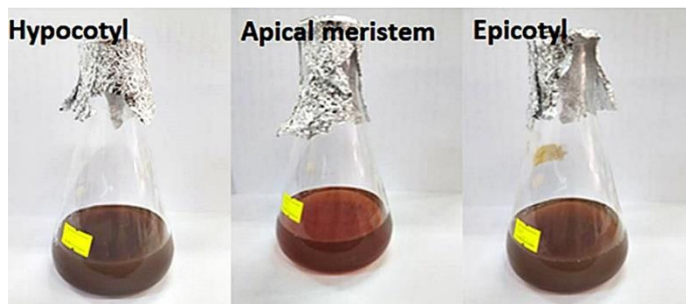


Fig. 3. The appearance of biosynthesized silver nanoparticles at 24°C with $1.96 \text{ mg L}^{-1} \text{ AgNO}_3 + 1 \text{ g}/10 \text{ ml}$ callus extracts after 48 hours.

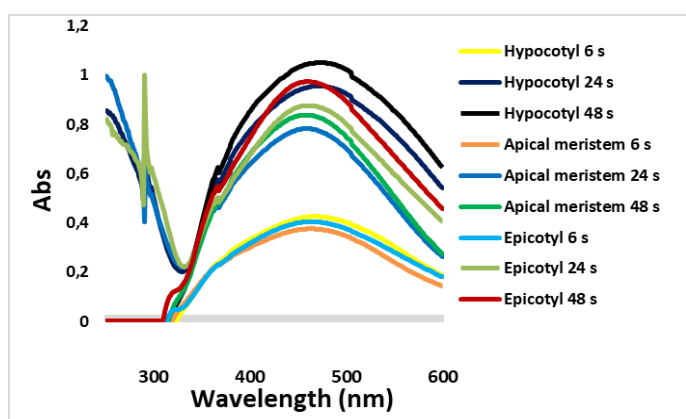


Fig. 4. UV-VIS spectrum of biosynthesized silver nanoparticles with $1.96 \text{ mg L}^{-1} \text{ AgNO}_3 + 1 \text{ g}/10 \text{ ml}$ callus extracts after 6, 24 and 48 hours.

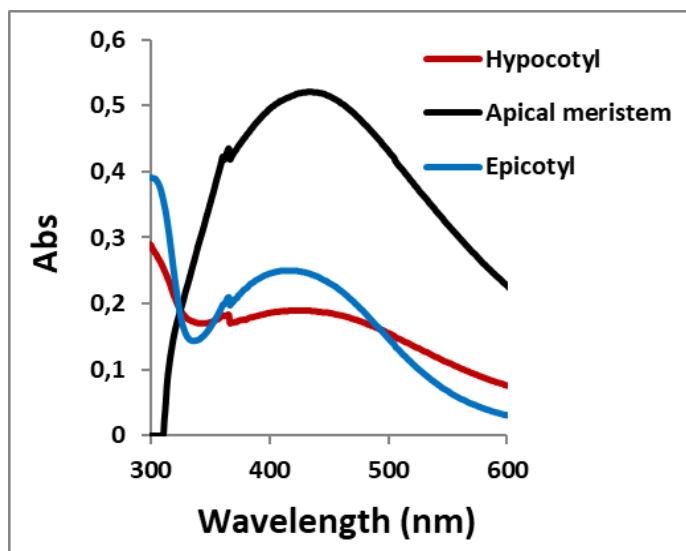


Fig. 5. UV-VIS spectrum of biosynthesized silver nanoparticles at 90°C with $1.96 \text{ mg L}^{-1} \text{ AgNO}_3 + 1 \text{ g}/10 \text{ ml}$ callus extracts.

AgNPs biosynthesis experiments were carried out separately at 40, 50, 60, 70, 80, 90, and 100°C temperatures with $1.96 \text{ mg L}^{-1} \text{ AgNO}_3 + 1 \text{ g}/10 \text{ ml}$ callus extracts (hypocotyl, apical meristem, and epicotyl). After 2 hours, a change in reaction color started. The change in the reaction color was observed the fastest in the samples kept at 90°C and the slowest

in the samples kept at 40°C . The highest biosynthesis was determined at 90°C . The biosynthesized AgNPs maximum absorbance was observed for hypocotyl, apical meristem, and epicotyl derived callus at 424, 436, and 417 nm wavelengths, respectively (Fig. 5).

AgNPs biosynthesis experiments were performed with $1.96 \text{ mg L}^{-1} \text{ AgNO}_3 + 1 \text{ g}/10 \text{ ml}$ callus extracts (hypocotyl, apical meristem, and epicotyl) at pH 5, 7, and 10. The change in reaction color started as soon as $1.96 \text{ mg L}^{-1} \text{ AgNO}_3$ was added. The most intense color change was seen at pH 5. Maximum absorbance in the UV spectrophotometer was observed for hypocotyl, apical meristem, and epicotyl derived callus at wavelengths of 456, 449, and 480 nm, respectively (Fig. 6).

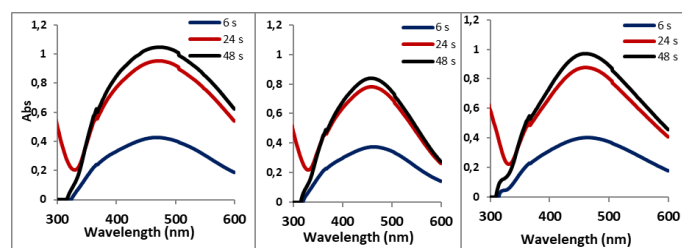


Fig. 6. UV-VIS spectrum of biosynthesized silver nanoparticles at pH: 5 with $1.96 \text{ mg L}^{-1} \text{ AgNO}_3 + 1 \text{ g}/10 \text{ ml}$ hypocotyl, apical meristem and epicotyl derived callus extracts after 6 hours.

3.3. TEM analysis of produced silver nanoparticles

TEM was applied to determine the morphology and size of AgNPs, which are biosynthesis products. Biosynthesized AgNPs from apical meristem derived calli were only evaluated by TEM analysis since the highest biosynthesis was determined in apical meristem derived calli for concentration, temperature, and pH experiments. Biosynthesized AgNPs, with $1.96 \text{ mg L}^{-1} \text{ AgNO}_3 + 1 \text{ g}/10 \text{ ml}$ callus extracts at room temperature had different shapes: triangular, elliptical, and spherical (Fig. 7a). AgNPs tend to aggregate. TEM analysis confirmed that it has an AgNP size distribution ranging from 18.25 to 37.8 nm.

Biosynthesized AgNPs from apical meristem derived calli at 90°C were found to be smaller in size and spherical in shape. TEM analysis confirmed that it has an AgNP size distribution ranging from 8.34-16.01 nm (Fig. 7b). AgNPs produced at 90°C were separated from each other and did not aggregate.

It was determined that AgNPs produced at pH:5 were spherical and elliptical. TEM analysis confirmed that it has an AgNP size distribution ranging from 10.67-37.85 nm (Fig. 7c).

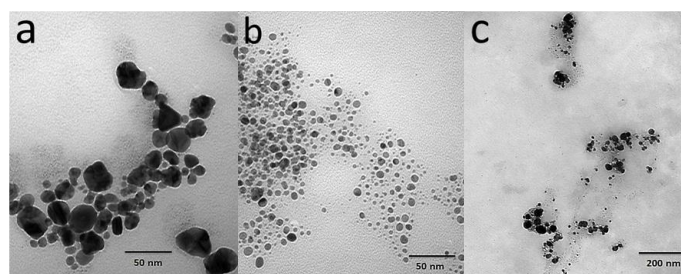


Fig. 7. Transmission electron microscopy micrographs of biosynthesized silver nanoparticles with apical meristem derived calli. a. $1.96 \text{ mg L}^{-1} \text{ AgNO}_3$, b. 90°C temperature, c. pH: 5.

3.4. XRD analysis of produced silver nanoparticles

The crystal structure of biosynthesized AgNPs with apical

meristem, hypocotyl, and epicotyl derived callus extracts was evaluated by XRD analysis. No 2θ peak was observed for biosynthesized AgNPs from the apical meristem and epicotyl calli at 90°C using a concentration of $1.96\text{ mg L}^{-1}\text{ AgNO}_3 + 1\text{ g/10 ml}$ callus extract. The 2θ peak was at 32.30° for AgNPs biosynthesize from hypocotyl calli. This (101) was attributed to the Miller indices (Fig. 8).

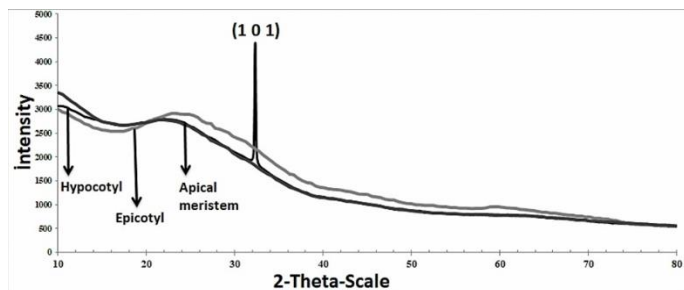


Fig. 8. XRD model of biosynthesized silver nanoparticles at 90°C with $1.96\text{ mg L}^{-1}\text{ AgNO}_3 + 1\text{ g/10 ml}$ hypocotyl, apical meristem and epicotyl derived callus extract.

For biosynthesized AgNPs at pH:5 using a concentration of $1.96\text{ mg L}^{-1}\text{ AgNO}_3 + 1\text{ g/10 ml}$ callus extract, the 2θ peaks were at 32.01° , 37.84° , 46.07° for the apical meristem. For hypocotyl: 32.55° , 38.35° , 46.52° . For epicotyl: 32.30° , 38.20° , 46.39° . These were attributed to the Miller indices (101), (111), and (200), respectively (Fig. 9).

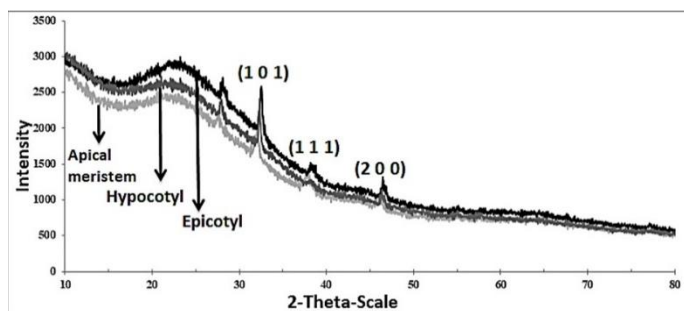


Fig. 9. XRD model of biosynthesized silver nanoparticles at pH:5 with $1.96\text{ mg L}^{-1}\text{ AgNO}_3 + 1\text{ g/10 ml}$ hypocotyl, apical meristem and epicotyl derived calli extract.

These peaks were caused by organic compounds present in the extract, which are responsible for the reduction of silver ions and stabilization of the resulting nanoparticles. The average crystal size of AgNPs was determined as 13.5 nm for biosynthesized AgNPs from apical meristem calli at 90°C , and 26 nm to medium at pH:5. It proved to be similar when compared with the TEM results.

3.5. FTIR analysis of produced silver nanoparticles

FTIR analysis was performed to identify possible organic biomolecules of hypocotyl, apical meristem and epicotyl derived callus extracts responsible for the biosynthesis of AgNPs. Absorption peaks in the FTIR spectrum of biosynthesized AgNPs from hypocotyl, apical meristem, and epicotyl derived callus extracts at 90°C using a concentration of $1.96\text{ mg L}^{-1}\text{ AgNO}_3 + 1\text{ g/10 ml}$ callus extract: for hypocotyl: 2913.7, 2856.5; for apical meristem: 2971.1, 2902.1; for epicotyl: 3257.2, 2964.7, 2918.8, 2859 cm^{-1} (Fig. 10). The strong absorption bands 2913.7, 2856.5, 2971.1, 2902.1, 3257.2, 2964.7, 2918.8, and 2859 cm^{-1} represent -CH stretching of the -

CH_3 and $-\text{CH}_2$ functional groups.

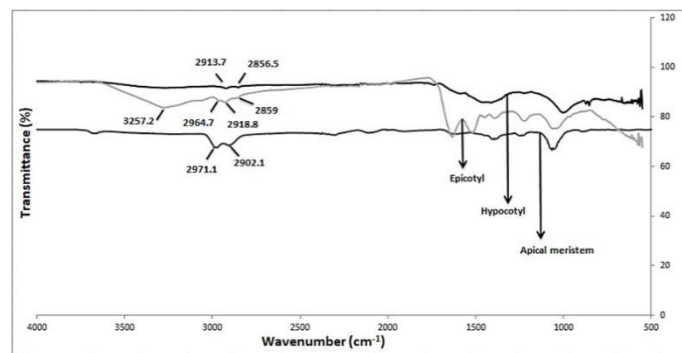


Fig. 10. FTIR spectrum of biosynthesized silver nanoparticles at 90°C condition with $1.96\text{ mg L}^{-1}\text{ AgNO}_3 + 1\text{ g/10 ml}$ hypocotyl, apical meristem and epicotyl derived calli extracts.

Absorption peaks in the FTIR spectrum of biosynthesized AgNPs from hypocotyl, apical meristem and epicotyl derived callus extracts at pH:5 using a concentration of $1.96\text{ mg L}^{-1}\text{ AgNO}_3 + 1\text{ g/10 ml}$ callus extract: for hypocotyl: 2921.7, 2859; for apical meristem: 2937.2, 2850; for epicotyl: 2930.2, 2853.3 cm^{-1} (Fig. 11).

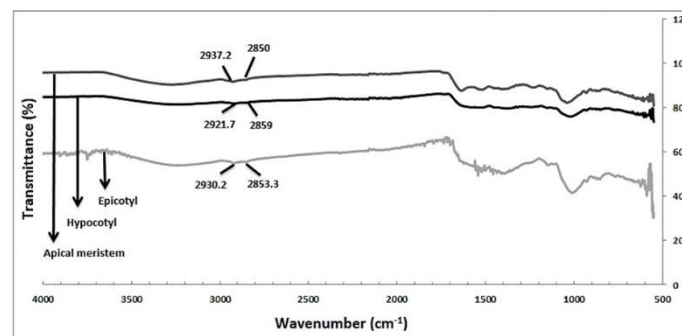


Fig. 11. FTIR spectrum of biosynthesized silver nanoparticles at pH:5 condition with $1.96\text{ mg L}^{-1}\text{ AgNO}_3 + 1\text{ g/10 ml}$ hypocotyl, apical meristem, and epicotyl derived calli extracts.

The strong absorption band at 2921.7, 2859, 2937.2, 2850, 2930.2, 2853.3 cm^{-1} represents the -CH stretching of the $-\text{CH}_3$ and $-\text{CH}_2$ functional groups (Sahayaraj et al., 2012; Mourdikoudis et al., 2018).

3.6. Determination of potential biological activity

Antibacterial activity: According to UV-Visible Spectrophotometer and XRD results, biosynthesized AgNPs using hypocotyl, apical meristem, and epicotyl calluses at pH: 5 were used for antibacterial activity experiments since the medium with the highest biosynthesis production was pH: 5. Hypocotyl, apical meristem and epicotyl calli without AgNPs were used as control group.

When the antibacterial test results were evaluated, no antibacterial activity was detected in the callus extracts (control group) that did not contain AgNP. However, no bacterial growth was observed in AgNP-hypocotyl (1.7mm), AgNP-apical meristem (1.2mm), and AgNP-epicotyl (1.6mm) zone diameters against Gram-positive *S. aureus* ATCC 25923 bacteria in AgNP-containing samples. Against Gram-negative *E. coli* CECT 4972 bacteria, no bacterial growth was observed in the zone diameters of AgNP- hypocotyl (1.0mm) and AgNP-epicotyl (1.1mm) (Fig. 12).

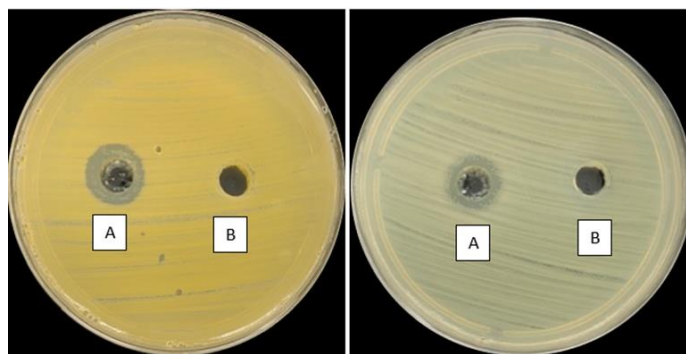


Fig. 12. Antibacterial effect by Agar-well cut diffusion method against *S. aureus* ATCC 25923 and *E. coli* CECT 4972 (A) AgNP-Epi (B) Epi

To increase the effectiveness of antibiotics used against *E. coli* bacteria and *S. aureus*, which are the most common microorganisms among the microorganisms that are the most common cause of hospital-acquired infections, 1 µg/µl AgNP used. Investigation of antibacterial activity of biosynthesized AgNPs against these bacteria was compared by determining the effect of control groups.

Considering the antibiotic effect against *S. aureus* ATCC 25923 bacteria, it was observed that 1 µg/µl was ineffective in many antibiotics except Oxacillin antibiotic, and it showed an effect against Nitrofurantoin antibiotic agent with a zone diameter of 18-22mm. We have found that Nitrofurantoin showed on 20-25mm (CLSI, 2020) inhibition zone to *E. coli*. In our opinion when the concentration of the biosynthesized AgNPs increases various influences may be done on antibacterial activity and at their use many areas might be grounded.

3.7. Determination of antioxidant activity

Hypocotyl, apical meristem, and epicotyl derived callus extracts were measured as the control group for DPPH and ABTS radical activity, and biosynthesized AgNPs from the callus extracts as the experimental group were measured. The results for biosynthesized AgNPs antioxidant activity are shown in Fig. 13.

The highest DPPH radical activity for extracts of control group-hypocotyl, apical meristem, and epicotyl derived callus was 52%, 48% and 49%, respectively; ABTS activity was 68%, 63%, 71%, respectively. DPPH radical activity for hypocotyl-AgNP; in concentration, temperature, and pH experiments: 55%, 41% and 46%, respectively; ABTS radical activity: 58%, 44% and 47%. DPPH radical activity for the apical meristem-AgNP; in concentration, temperature, and pH experiments: 65%, 39% and 41%, respectively; ABTS radical activity: 63%, 47% and 54%. DPPH radical activity for epicotyl-AgNP; in concentration, temperature and pH experiments: 53%, 44% and 49%, respectively; ABTS radical activity: 58%, 49% and 56% (Fig. 13) (Table 1).

4. Discussion

Plant tissue cultures are important for production of secondary metabolites. Plant growth regulators in different combinations or in different concentrations are used to increase the concentrations of secondary metabolites in calli (Jakovljević et al., 2022; Ozyigit et al., 2023). Since in our previous study, the highest secondary metabolite production occurred in the MS medium containing kinetin (1.5 mg L⁻¹), NAA (1.5 mg L⁻¹) and 2,4-D (0.7 mg L⁻¹) (Colgecen et al., 2014). So, to callus production was used in the same medium for this study. The first

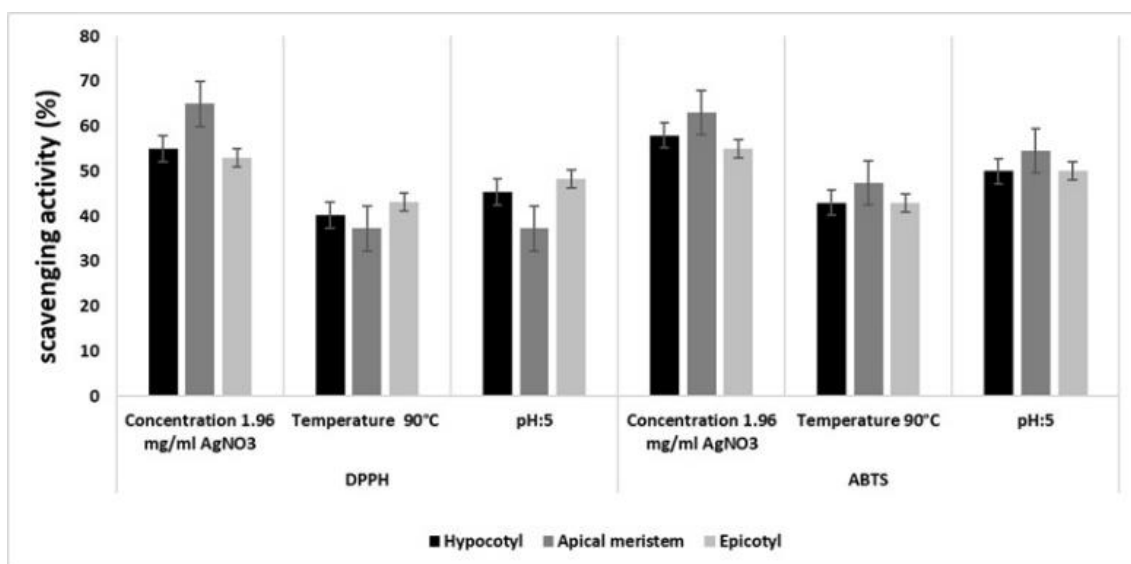


Fig. 13. Antioxidant activity of biosynthesized silver nanoparticles at 1.96 mg L⁻¹ AgNO₃, 90°C and pH:5 conditions (a) hypocotyl, (b) apical meristem, (c) epicotyl.

Table 1

The effect on antioxidant activity of biosynthesized silver nanoparticles by callus extracts (p<0.05).

The Biosynthesized Silver Nanoparticles	Hypocotyl		Apical Meristem		Epicotyl	
	DPPH	ABTS	DPPH	ABTS	DPPH	ABTS
Concentration (1.96 mg L ⁻¹ AgNO ₃)	46.00±1.76	49.40±3.42	50.00±5.40	49.50±4.94	44.70±3.76	48.75±2.83
Temperature (90°C)	38.75±1.03	41.75±1.03	37.00±0.80	42.00±1.77	41.50±1.03	41.75±1.03
pH:5	42.50±2.48	47.00±2.48	38.50±1.50	45.75±3.49	45.75±2.48	47.00±2.48

Mean ± SE

callus formation occurred after 1 week. After 4 weeks, the calli were taken to the second subculture.

In our study, at different concentrations of AgNO_3 (0.16, 0.5, 0.84, 1.18, 1.52 and 1.96 mg L^{-1}), different temperatures (40, 50, 60, 70, 80, 90, 100°C) and different pH (5, 7, 10) experiments, a change was observed in callus cultures of natural tetraploid *T. pratense* L. Since the bioreducing agents in the extracts are important and primary source in reducing Ag^+ ions to Ag^0 particles (Chowdhury et al., 2008; Vijayaraghavan et al., 2012; Rodríguez-León et al., 2013; Firoozi et al., 2016; Malik et al., 2022), the color transformation observed in our study was attributed to a reduction mechanism.

In terms of reduction time, reduction (Ag^+ to Ag^0) started in 6 hours in terms of color change with the addition of AgNO_3 to callus and cell suspension culture extracts in concentration and temperature experiments in our study, while reduction started as soon as AgNO_3 was added in terms of color change in pH trials. It was concluded that the recording of different reduction times in different conditions depends on the changes in the amount of metabolites in the herb and *in vitro* samples, the temperature and pH of the environment (Raja et al., 2012; Manosalva et al., 2019; Bernabé-Antonio et al., 2022). In our study, the reduction time, which is 4-6 hours under concentration, temperature, and pH conditions, is similar to our study according to the literature (Patra et al., 2015; Labulo et al., 2016; Jalab et al., 2021). Some literatures do not give a reduction period, since the time at which the reduction begins is important, not giving the reduction period is seen as a deficiency (Sathiya and Akilandeswari, 2014). In our study, we have given the onset of reduction and the stability of the color in accordance with much literature. Also, preliminary experiments were carried out at 200-800 nm wavelength to determine the UV-VIS spectrum range of biosynthesized AgNPs using extracts of callus of natural tetraploid *T. pratense* L. According to the results, it was determined that the wavelength of 300-600 nm was sufficient for the absorbance range of AgNPs, and the studies were continued in the range of 300-600 nm (Mude et al., 2009; Nabikhan et al., 2010; Netala et al., 2015; Solanki et al., 2021; Alfarraj et al., 2023). For ultraviolet-violet spectroscopy, similar results were determined in the studies of some researchers. Aref and Salem (2020) observed the maximum absorbance for biosynthesized AgNPs with *Cinnamomum camphora* callus extract is at 420 nm, Botcha and Prattipat (2020) observed the maximum absorbance is at 447 nm for the biosynthesized AgNPs with *Hyptis suaveolens* callus extract, Lashin et al. (2021) observed maximum absorbance at 440 nm for biosynthesized AgNPs by *Solanum incanum* L. callus extract.

AgNPs formation was interpreted according to the results of UV-VIS spectra using callus extracts of the natural tetraploid *T. pratense* L. (1 g/10 ml) + AgNO_3 (0.16, 0.5, 0.84, 1.18, 1.52 and 1.96 mg L^{-1}) salt at different concentrations. It was determined that the absorbance peak shifted towards the shorter wavelength region (blue) as the AgNO_3 concentration increased. As a result of our experiments, we continued the experiments with 1.96 mg L^{-1} AgNO_3 at different temperatures and pH intervals by using the extracts of callus cultures.

A lower temperature was seen as a slower increase in the absorption band. It was concluded that the rate of nanostructure formation is importantly dependent on temperature. Yeshchenko et al. (2013) suggested that higher temperatures increase the activation energy of molecules, thus leading to a faster reaction rate.

Studies have shown that the size, morphology, stability,

and chemical-physical properties of metal nanoparticles are affected by experimental conditions (extract or salt concentration, temperature, and pH), the interaction of metal ions with reducing agents, and absorption processes (Ghorbani et al., 2011). In general, control of the shape, size, and distribution of the produced nanoparticles; synthesis methods are achieved by changing reducing and stabilizing factors. Since the optical, electronic, magnetic, and catalytic properties of nanoparticles depend on their size, shape, and chemical-physical properties, the size and shape of AgNPs are quite important for some experiments, so few studies focus specifically on the size and shape of AgNPs (He et al., 2004; Khodashenas and Ghorbani, 2019; Restrepo and Villa, 2021).

The size and shape of AgNPs are generally evaluated by TEM analysis, however, it is also known that the broadening or narrowing of the UV-VIS spectrum band is a wider nanoparticle size range and amount in solution (Nikaeen et al., 2020; Chowdhury et al., 2021). In our study, the peaks in the absorption band in the UV-VIS spectrum of AgNPs biosynthesized under different conditions using callus extracts were wider for concentration trials, while they were narrower for temperature and pH studies. According to the results obtained, when all samples are examined, AgNPs seen in TEM micrographs support the UV-VIS spectrum results in terms of size and shape. It was concluded that AgNPs were affected by different conditions, with different sizes of AgNPs biosynthesized under different conditions in concentration (1.96 mg L^{-1} AgNO_3 + 1 g/10 ml), temperature: 90°C and pH: 5 experiments according to TEM micrographs. This suggested that AgNPs were covered by biomolecules such as primary and secondary metabolites in the extracts and was confirmed by studies by different researchers (Lu et al., 2014; Roy et al., 2019; Baran et al., 2023).

When compare the DPPH and ABTS reporting, ABTS was confirmed to have significantly higher ($p < 0.05$) scavenging activity. According to some researchers, it has been reported that the antioxidant activity of biosynthesized AgNPs is due to the presence of terpenoids, phenolic compounds, and flavonoids, which allows them to act as hydrogen donors and reducing agents in plants (Bedlovičová et al., 2020).

5. Conclusion

In the current study, biosynthesized AgNPs using the extract of hypocotyl, apical meristem, and epicotyl derived callus extracts were reported using callus extract of natural tetraploid *Trifolium pratense* L. for the first time. Characterization of AgNPs was performed using UV-vis, TEM, XRD, and FTIR analysis, and results revealed that different concentrations of callus extract did not affect the performance of the prepared nanoparticles as well as crystallinity. The biosynthesized AgNPs were triangular, elliptical, and spherical in shape and determined by TEM, and XRD. In the current study, green biosynthesis of AgNPs was performed antimicrobial activity and antioxidant activity of AgNPs were evaluated, and the result revealed that AgNPs have potential antimicrobial activity against *E. coli* bacteria and *S. aureus*. Moreover, biosynthesized AgNPs have strong antioxidant activity as well as antimicrobial activity in safe use. In summary, these findings underscore the potential of biotechnological strategies in green nanotechnology, which can be offered for developing metal nanoparticles with potential biomedicine and biotechnology applications. Additionally, biosynthesized

AgNPs can be offered as an alternative solution to seed surface sterilization, or AgNPs can be recommended for seeds with low germination percentages based on the positive effect of AgNPs on seed germination. On the other hand, biosynthesized AgNPs can be a solution in studies such as increasing the shelf life of foods, contamination problems of medical devices, developing antibiotics against resistant bacteria, and increasing the effectiveness of active substances used in cancer research.

Acknowledgements: The research project was supported by Zonguldak Bulent Ecevit University, Science Research Project

References

- Ahmad, N., Muhammad, J., Khan, K., Ali, W., Fazal, H., Ali, M., ... & Hano, C. (2022). Silver and gold nanoparticles induced differential antimicrobial potential in calli cultures of *Prunella vulgaris*. *BMC chemistry*, 16(1), 20.
- Aktepe, N. (2021). Synthesis, characterization and antimicrobial activities of silver nanomaterials. *DÜMF Mühendislik Dergisi*, 12(2), 347-354.
- Alfarraj, N. S., Tarrowm, M., Al-Qurainy, F., Nadeem, M., Khan, S., Salih, A. M., ... & Perveen, K. (2023). Biosynthesis of Silver Nanoparticles and Exploring Their Potential of Reducing the Contamination of the In Vitro Culture Media and Inducing the Callus Growth of *Rumex nervosus* Explants. *Molecules*, 28(9), 3666.
- Allawadhi, P., Singh, V., Khurana, A., Khurana, I., Allawadhi, S., Kumar, P., ... & Bharani, K. K. (2021). Silver nanoparticle based multifunctional approach for combating COVID-19. *Sensors International*, 2, 100101.
- Anjum, S., & Abbasi, B. H. (2016). Thidiazuron-enhanced biosynthesis and antimicrobial efficacy of silver nanoparticles via improving phytochemical reducing potential in callus culture of *Linum usitatissimum* L.. *International Journal of Nanomedicine*, 11, 715-728.
- Aref, M. S., & Salem, S. S. (2020). Bio-callus synthesis of silver nanoparticles, characterization, and antibacterial activities via *Cinnamomum camphora* callus culture. *Biocatalysis and Agricultural Biotechnology*, 27, 101689.
- Arsène, M. M. J., Podoprigora, I. V., Davares, A. K. L., Razan, M., Das, M. S., & Senyagin, A. N. (2021). Antibacterial activity of grapefruit peel extracts and green-synthesized silver nanoparticles. *Veterinary World*, 14(5), 1330-1341.
- Avcioglu, F., Behçet, M., Karabork, S., & Kurtoglu, M. G. (2019). Yara örneklerinden izole edilen Mikroorganizmaların Antimikrobiyal direnç oranları-üç yıllık değerlendirme. *Düzce Üniversitesi Sağlık Bilimleri Enstitüsü Dergisi*, 9(3), 110-114.
- Labulo, A. H., Adesuji, E. T., Dedeke, O. A., Bodede, O. S., Oseghale, C. O., Moodley, R., ... & Adegoke, O. A. (2016). A dual-purpose silver nanoparticles biosynthesized using aqueous leaf extract of *Detarium microcarpum*: an under-utilized species. *Talanta*, 160, 735-744.
- Aziz, M. S. A., Shaheen, M. S., Nekeety, A. A., & Wahhab, M. A. A. (2014). Antioxidant and antibacterial activity of silver nanoparticles biosynthesized using *Chenopodium murale* leaf extract. *Journal of Saudi Chemical Society*, 18, 356-363.
- Baran, M. F., Keskin, C., Baran, A., Hatipoğlu, A., Yildiztekin, M., Küçükaydın, S., ... & Eftekhari, A. (2023). Green synthesis of silver nanoparticles from *Allium cepa* L. Peel extract, their antioxidant, antipathogenic, and anticholinesterase activity. *Molecules*, 28(5), 2310.
- Baruah, K., Haque, M., Langbang, L., Das, S., Aguan, K., & Roy, A.S. (2021). *Ocimum sanctum* mediated green synthesis of silver nanoparticles: A biophysical study towards lysozyme binding and antibacterial activity. *Journal of Molecular Liquids*, 337, 116422.
- Bedlovičová, Z., Strapáč, I., Baláž, M., & Salayová, A. (2020). A brief overview on antioxidant activity determination of silver nanoparticles. *Molecules*, 25(14), 3191.
- Bernabé-Antonio, A., Martínez-Ceja, A., Romero-Estrada, A., Sánchez-Carranza, J. N., Columba-Palomares, M. C., Rodríguez-López, V., ... & Gutiérrez-Hernández, J. M. (2022). Green synthesis of silver nanoparticles using *Randia aculeata* L. cell culture extracts, characterization, and evaluation of antibacterial and antiproliferative Activity. *Nanomaterials*, 12(23), 4184.
- Botcha, S., & Prattipati, S. D. (2020). Callus extract mediated green synthesis of silver nanoparticles, their characterization and cytotoxicity evaluation against MDA-MB-231 and PC-3 cells. *BioNanoScience*, 10, 11-22.
- Buyukkartal, H. N., & Colgecen, H. (2007). The reasons of sterility during pollen grain formation in the natural tetraploid *Trifolium pratense* L. *International Journal of Botany*, 3(2), 188-195.
- Chowdhury, M. H., Ray, K., Geddes, C. D., & Lakowicz, J. R. (2008). Use of silver nanoparticles to enhance surface plasmon-coupled emission (SPCE). *Chemical Physics Letters* 452, 162-167.
- Chowdhury, R. A., Dhar, S. A., Das, S., Nahian, K., & Qadir, R. (2021). Green synthesis and characterization of silver nanoparticles from the aqueous extract of the leaves of *Citrus aurantifolia*. *Materials Today: Proceedings*, 44, 1039-1042.
- CLSI, (2020). Performance standards for antimicrobial susceptibility testing. 30th ed. CLSI supplement M100. Wayne, PA: Clinical and Laboratory Standards Institute.
- Colgecen, H., Caliskan, U., Kartal, M., & Buyukkartal, H. N. (2014). Comprehensive evaluation of phytoestrogen accumulation in plants and *in vitro* cultures of *Medicago sativa* L. 'Elçi' and natural tetraploid *Trifolium pratense* L.. *Turkish Journal of Biology*, 38, 619-627.
- Dakal, T. C., Kumar, A., Majumdar, R. S., & Yadav, V. (2016). Mechanistic basis of antimicrobial actions of silver nanoparticles. *Frontiers in Microbiology*, 16(7), 1831.
- Das, G., Shin, H., & Patra, J. K. (2020). Comparative assessment of antioxidant, anti-diabetic and cytotoxic effects of three peel/shell food waste extract-mediated silver nanoparticles. *International Journal of Nanomedicine*, 15, 9075-9088.
- Devi, M. P. I., Nallamuthu, N., Rajini, N., Rajulub, A. V., Ramc, N. H., & Siengchin, S. (2018). Cellulose hybrid nanocomposites using Napier grass fibers with in situ generated silver nanoparticles as fillers for antibacterial applications. *International Journal of Biological Macromolecules*, 118, 99-106.
- Duncan, D. B. (1955). Multiple range and multiple F-test. *Biometrics*, 11, 1-42.
- Elci, S. (1982). The utilization of genetic resource in fodder crop breeding, *Eucarpia*. Fodder Crop Section, September, Aberystwyth, UK, 1-347.
- Ellnain-Wojtaszek, M., Kruczynski, Z., & Kasprzak, J. (2003). Investigation of the free radical scavenging activity of *Ginkgo biloba* L. leaves. *Fitoterapia*, 74, 1-6.
- EUCAST, (2014). Antimikrobik duyarlılık testine yönelik disk difüzyon yöntemi Sürüm.
- Fierascu, I., Bunghez, I. R., Fierascu, R., Ion, R. M., Dinu-Pîrvu, C. E., & Nuță, D. (2014). Characterization and Antioxidant Activity of Phytosynthesized Silver Nanoparticles Using *Calendula officinalis* Extract. *Farmacia*, 62, 1.
- Firoozi, S., Jamzad, M., & Yari, M. (2016). Biologically synthesized silver nanoparticles by aqueous extract of *Satureja intermedia* C.A. Mey and the evaluation of total phenolic and flavonoid contents and antioxidant activity. *Journal of Nanostructure in Chemistry*, 6, 357-364.
- Gharari, Z., Hanachi, P., Sadeghinia, H., Walker, T. R. (2022). *Cichorium intybus* bio-callus synthesized silver nanoparticles: A promising antioxidant, antibacterial and anticancer compound. *International Journal of Pharmaceutics*, 625, 122062.
- Ghorbani, H. R., Safekordi, A. A., Attar, H., & Rezayat Sorkhabadi, S. M. (2011). Biological and non-biological methods for silver nanoparticles synthesis. *Chemical and Biochemical Engineering Quarterly*, 25(3), 317-326.
- Gonzalez-Carter, D. A., Leo, B. F., Ruenraroengsak, P., Chen, S., Goode, A. E., Theodorou, I. G., ... & Porter, A. E. (2017). Silver nanoparticles

- reduce brain inflammation and related neurotoxicity through induction of H2S-synthesizing enzymes. *Scientific reports*, 7(1), 42871.
- He, B., Tan, J., Liew, K., & Liu, H. (2004). Synthesis of size controlled ag nanoparticles. *Journal of Molecular Catalysis A: Chemical*, 221, 121-126.
- Iashin, I., Hasanin, M., & Hassan, S. A. M. (2023). Green biosynthesis of zinc and selenium oxide nanoparticles using callus extract of *Ziziphus spina-christi*: characterization, antimicrobial, and antioxidant activity. *Biomass Conv. Bioref*, 13, 10133-10146.
- Jakovljević, D., Stanković, M., & Warchoń, M. (2022). Basil (*Ocimum L.*) cell and organ culture for the secondary metabolites production: a review. *Plant Cell Tissue Organ Culture*, 149, 61-79.
- Jalab, J., Abdelwahed, W., Kitaz, A., & Al-Kayali, R. (2021). Green synthesis of silver nanoparticles using aqueous extract of *Acacia cyanophylla* and its antibacterial activity. *Heliyon*, 7(9), e08033.
- Jeremiah, S. S., Miyakawa, K., Morita, T., Yamaoka, Y., & Ryo, A. (2020). Potent antiviral effect of silver nanoparticles on SARS-CoV-2. *Biochemical and Biophysical Research Communications*, 533, 195-200.
- Khodashenas, B., & Ghorbani, H. R. (2019). Synthesis of silver nanoparticles with different shapes. *Arabian Journal of Chemistry*, 12(8), 1823-1838.
- Khaosaad, T., Krenn, L., Medjakovic, S., Ranner, A., Lossl, A., Nell, M., Jungbauer, A., & Vierheilig, H. (2008). Effect of mycorrhization on the isoflavone content and the phytoestrogen activity of red clover. *Journal of Plant Physiology*, 165, 1161-1167.
- Kumar, K. S., & Kathireswari, P. (2016). Biological synthesis of silver nanoparticles (Ag-NPS) by *Lawsonia inermis* (Henna) plant aqueous extract and its antimicrobial activity against human pathogens. *International Journal of Current Microbiology and Applied Sciences*, 5(3), 926-937.
- Lashin, I., Fouda, A., Gobouri, A. A., Azab, E., Mohammedsalem, Z. M., & Makhariha, R. R. (2021). Antimicrobial and *in vitro* cytotoxic efficacy of biogenic silver nanoparticles (Ag-NPs) fabricated by callus extract of *Solanum incanum L.* *Biomolecules*, 11, 341.
- Li, W. R., Xie, X. B., & Shi, Q. S. (2011). Antibacterial effect of silver nanoparticles on *Staphylococcus aureus*. *Biomaterials*, 24, 135-141.
- Lu, F., Gao, Y., Huang, J., Sun, D., & Li, Q. (2014). Roles of biomolecules in the biosynthesis of silver nanoparticles: case of *Gardenia jasminoides* extract. *Chinese Journal of Chemical Engineering*, 22, 706-712.
- Malik, M., Iqbal, M. A., Malik, M., Raza, M. A., Shahid, W., Choi, J. R., & Pham, P. V. (2022). Biosynthesis and characterizations of silver nanoparticles from *Annona squamosa* leaf and fruit extracts for size-dependent biomedical applications. *Nanomaterials*, 12(4), 616.
- Manosalva, N., Tortella, G., Cristina Diez, M., Schalchli, H., Seabra, A. B., Durán, N., & Rubilar, O. (2019). Green synthesis of silver nanoparticles: effect of synthesis reaction parameters on antimicrobial activity. *World Journal of Microbiology and Biotechnology*, 35, 88.
- Moldovan, B., David, L., Achim, M., Clichici, S., & Filip, G.A. (2016). A green approach to phytomediated synthesis of silver nanoparticles using *Sambucus nigra L.* fruits extract and their antioxidant activity. *Journal of Molecular Liquids*, 221, 271-278.
- Mourdikoudis, S., Pallares, R. M., & Thanh, N. T. K. (2018). Characterization techniques for nanoparticles: comparison and complementarity upon studying nanoparticle properties. *Nanoscale*, 10, 12871-12934.
- Mude, N., Ingle, A., Gade, A., & Rai, M. (2009). Synthesis of silver nanoparticles using callus extract of *Carica papaya*-A first report. *Journal of Plant Biochemistry and Biotechnology*, 18(1), 83-86.
- Murashige, T., & Skoog, F. (1962). A revised medium for rapid growth and bioassay with tobacco tissue cultures. *Physiologia Plantarum*, 15, 473-497.
- Nabikhan, A., Kandasamy, K., Raj, A., & Alikunhi, N. M. (2010). Synthesis of antimicrobial silver nanoparticles by callus and leaf extracts from saltmarsh plant, *Sesuvium portulacastrum L.* *Colloids and Surfaces B: Biointerfaces*, 79, 488-493.
- Netala, V. N., Kotakadi, V. S., Nagam, V., Bobbu, P., Ghosh, S. B., & Tarte, V. (2015). First report of biomimetic synthesis of silver nanoparticles using aqueous callus extract of *Centella asiatica* and their antimicrobial activity. *Applied Nanoscience*, 5, 801-807.
- Nikaen, G., Yousefinejad, S., Rahmdel, S., Samari, F., & Mahdavinia, S. (2020). Central composite design for optimizing the biosynthesis of silver nanoparticles using *Plantago major* extract and investigating antibacterial, antifungal and antioxidant activity. *Scientific Reports*, 10, 9642.
- Ochoa-Villarreal, M., Howat, S., Hong, S., Jang, M. O., Jin, Y. W., Lee, E. K., & Loake, G. J. (2016). Plant cell culture strategies for the production of natural products. *BMB Reports*, 49(3), 149.
- Ozturk Kup, F., Coskuncay, S., & Duman, F. (2020). Biosynthesis of silver nanoparticles using leaf extract of *Aesculus hippocastanum* (horse chestnut): Evaluation of their antibacterial, antioxidant and drug release system activities. *Materials Science and Engineering: C*, 107, 110207.
- Ozyigit, I. I., Dogan, I., Hocaoglu-Ozyigit, A., Yalcin, B., Erdogan, A., Yalcin, I. E., ... & Kaya, Y. (2023). Production of secondary metabolites using tissue culture-based biotechnological applications. *Frontiers in Plant Science*, 14, 1132555.
- Pandit, R. (2015). Green synthesis of silver nanoparticles from seed extract of *Brassica nigra* and its antibacterial activity. *Nusantara Bioscience*, 7 (1), 15-19.
- Patra, S., Mukherjee, S., Barui, A. K., Ganguly, A., Sreedhar, B., & Patra, C. R. (2015). Green synthesis, characterization of gold and silver nanoparticles and their potential application for cancer therapeutics. *Materials Science and Engineering: C*, 53, 298-309.
- Raja, K., Saravanakumar, A., & Vijayakumar, R. (2012). Efficient synthesis of silver nanoparticles from *Prosopis juliflora* leaf extract and its antimicrobial activity using sewage. *Spectrochimica Acta Part A: Molecular and Biomolecular Spectroscopy*, 97, 490-494.
- Rakesh, B., Srinatha, N., Rudresh Kumar, K. J., Madhu, A., Suresh Kumar, M. R., & Praveen, N. (2022). Antibacterial activity and spectroscopic characteristics of silver nanoparticles synthesized via plant and *in vitro* leaf-derived callus extracts of *Mucuna pruriens* (L.) DC.. *South African Journal of Botany*, 148, 251-258.
- Restrepo, C. V., & Villa, C. C. (2021). Synthesis of silver nanoparticles, influence of capping agents, and dependence on size and shape: a review. *Environmental Nanotechnology, Monitoring & Management*, 15, 100428.
- Rodríguez-León, E., Iñiguez-Palomares, R., Navarro, R. E., Herrera-Urbina, R., Tánori, J., Iñiguez-Palomares, C., & Maldonado, A. (2013). Synthesis of silver nanoparticles using reducing agents obtained from natural sources (*Rumex hymenosepalus* Extracts). *Nanoscale Research Letters*, 8, 318.
- Roy, A., Bulut, O., Some, S., Mandal, A. K., & Yilmaz, M. D. (2019). Green synthesis of silver nanoparticles: biomolecule-nanoparticle organizations targeting antimicrobial activity. *RSC Advances*, 9, 2673-2702.
- Sahayaraj, K., Rajesh, S., & Rathi, J. M. (2012). Silver nanoparticles biosynthesis using marine alga *Padina pavonica* (Linn.) and its microbicidal activity. *Digest Journal of Nanomaterials and Biostructures*, 7(4), 1557-1567.
- Salem, S. S., & Fouda, A. (2021). Green synthesis of metallic nanoparticles and their prospective biotechnological applications: an overview. *Biological Trace Element Research*, 199, 344-370.
- Sathiya, C. K., & Akilandeswari, S. (2014). Fabrication and characterization of silver nanoparticles using *delonix elata* leaf Broth. *Spectrochimica Acta Part A: Molecular and Biomolecular Spectroscopy*, 128, 337-341.
- Sharifi-Rad, M., Pohl, P., Epifano, F., & Álvarez-Suarez, J. M. (2020). Green synthesis of silver nanoparticles using *Astragalus tribuloides* delile. root extract: characterization, antioxidant, antibacterial, and anti-inflammatory activities. *Nanomaterials*, 10, 2383.
- Sharifi-Rad, M., Pohl, P., & Epifano, F. (2021). Phytofabrication of silver nanoparticles (agnps) with pharmaceutical capabilities using *Otostegia persica* (Burm.) Boiss. leaf extract. *Nanomaterials*, 11(4), 1045.
- Singh, P., Kim, Y. J., Zhang, D., & Yang, D. C. (2016). Biological synthesis of nanoparticles from plants and microorganisms. *Trends in Biotechnology*, 34, 7.
- Snedecor, G. W., Cochran, W. G. (1967). Statistical methods. Iowa, USA: The Iowa State University Press, 327-329.
- Solanki, A., Rathod, D., Patel, I. C., & Panigrahi, J. (2021). Impact of silver nanoparticles as antibacterial agent derived from leaf and callus of *Celastrus paniculatus* Willd. *Future Journal of Pharmaceutical Sciences*, 7, 60-69.
- Szydłowska-Czeraniak, A., Tulodziecka, A., & Szlyk, E. (2012). A silver nanoparticle-based method for determination of antioxidant capacity of rapeseed and its products. *Analyst*, 137, 3750.
- Tian, X., Jiang, X., Welch, C., Croley, T. R., Wong, T. Y., Chen, C., & Yin, J. J. (2018). Bactericidal effects of silver nanoparticles on *Lactobacilli*

- and the underlying mechanism. *ACS Applied Materials & Interfaces*, 10, 8443-8450.
- Vijayaraghavan, K., Kamala Nalini, S. P., Udaya Prakash, N., & Madhankumar, D. (2012). Biomimetic synthesis of silver nanoparticles by aqueous extract of *Syzygium aromaticum*. *Colloids and Surfaces B: Biointerfaces*, 94, 114-117.
- Wang, C. K., & Lee, W. H. (1996). Separation, Characteristics, and Biological Activities of Phenolics in Areca Fruit. *Journal of Agriculture and Food Chemistry*, 44(8), 1-6.
- WHO, (2019). World Health Organization. New report calls for urgent action to avert antimicrobial resistance crisis. Joint News Release, 1-29.
- Xia, Q. H., Ma, Y. J., & Wang, J. W. (2016). Biosynthesis of silver nanoparticles using *Taxus yunnanensis* callus and their antibacterial activity and cytotoxicity in human cancer cells. *Nanomaterials*, 6, 160.
- Yeshchenko, O. A., Dmitruk, I. M., Alexeenko, A. A., Kotko, A. V., Verdal, J., & Pinchuk, A. O. (2013). Temperature dependence of the surface plasmon resonance in gold nanoparticles. *Surface Science*, 608, 275-281.
- Yugay, Y. A., Sorokina, M. R., Grigorchuk, V. P., Rusapetova, T. V., Silant'ev, V. E., Egorova, A. E., ... & Shkryl, Y. N. (2023). Biosynthesis of Functional Silver Nanoparticles Using Callus and Hairy Root Cultures of *Aristolochia manshuriensis*. *Journal of Functional Biomaterials*, 14(9), 451.
- Yurttas, E., Tetik, N., & Ayrilmis, N. (2022). Antimicrobial properties of 3D printed biocomposites with heat-treated wood flour using silver nanoparticles with leaf extract. *Wood Material Science and Engineering*, 18(2), 663-671.

Cite as: Karahan, H., Tetik, N., & Colgecen, H. (2023). Phytofabrication of silver nanoparticles using callus extract of natural tetraploid *Trifolium pratense* L. and its bioactivities. *Front Life Sci RT*, 4(SI), 18-28.